Chinese Chemical Letters 31 (2020) 1133–1136

Contents lists available at ScienceDirect

Chinese Chemical Letters

journal homepage: www.elsevier.com/locate/cclet

Communication

Ag@Au core/shell triangular nanoplates with dual enzyme-like properties for the colorimetric sensing of glucose

Ao Liu[a], Mengmeng Li[a], Jingxiang Wang[b], Fan Feng[a], Yu Zhang[a], Zhiwei Qiu[a], Yuzhu Chen[a], Benjamin Edem Meteku[a], Congying Wen[a], Zifeng Yan[c], Jingbin Zeng[a,d,*]

[a] College of Science, China University of Petroleum (East China), Qingdao 266580, China
[b] Integrated Traditional Chinese and Western Medicine Hospital of Shandong, Qingdao 266002, China
[c] State Key Laboratory of Heavy Oil Processing, China University of Petroleum (East China), Qingdao 266580, China
[d] State Key Laboratory of Chemo/Biosensing and Chemometrics, Hunan University, Changsha 410082, China

ARTICLE INFO

Article history:
Received 23 August 2019
Received in revised form 11 October 2019
Accepted 11 October 2019
Available online 21 October 2019

Keywords:
Nanozyme Ag@Au core/shell
Nanoplates
Etching glucose
Colorimetric sensing

ABSTRACT

Due to the serious harm of diabetes to human health, development of sensitive assays for glucose level is of high significance for early prevention and treatment of diabetes. Currently, most conventional enzyme-based glucose sensors suffer from high cost and low stability due to the inherent defects of natural enzymes. Herein, we develop a pure nanozyme-based glucose detection method using Ag@Au core/shell triangular nanoplates (TNPs), which combines glucose oxidase (GOD)- and horseradish peroxidase (HRP)-like activities of the Au shell and inherent plasmonic properties of Ag TNPs. The sensing mechanism is based on the fact that the Au shell possessed GOD-like activity, enabling the oxidation of glucose to produce H_2O_2, which can further etch the silver core, leading to the decrease of absorbance at 800 nm and the color change from blue to colorless. Compared with the previous nanozymes-based glucose sensors, our method avoids the use of enzymes and organic chromogenic agent. Moreover, the stability of the Ag@Au core/shell TNPs is much better than that of Ag TNPs due to the protection by the coating of the Au shell. This method was successfully applied to the detection of urine samples from patients with diabetes, indicating its practical applicability for real sample analysis.
© 2019 Chinese Chemical Society and Institute of Materia Medica, Chinese Academy of Medical Sciences. Published by Elsevier B.V. All rights reserved.

Diabetes is a metabolic disease with the characteristic of disordered metabolism and hyperglycemia, which causes chronic damage and dysfunction of various tissues in human body [1–5]. The change of glucose level in human body can reflect the status of sugar metabolism in the body, and the measurement of glucose content is an important evidence to judge whether people have diabetes [6]. Thus, the rapid and sensitive detection of glucose is of great significance for the prevention and treatment of diabetes.

To date, much attention has been focused on the development of simple, low-cost, and accurate glucose sensors. At present, electrochemical enzyme-biosensors [7,8] and colorimetric enzyme-biosensors [9] have been extensively studied for the measurement of glucose, and some of such sensors have already been commercialized for diabetic patients. Combining the horseradish peroxidase (HRP) and glucose oxidase (GOD) with the paper-based biosensors, Chen and coworkers developed a simple and rapid colorimetric method for the detection of glucose [10]. Although biological enzyme has the advantages of high catalytic activity and substrate specificity, they always suffer from intrinsic shortcomings such as high cost, low operational stability, and difficulty in storage [11]. In order to overcome these defects, researchers have devoted to the exploration of mimetic enzyme for a long time. With the development of nanomaterials, nanozymes are widely used as substitutes of biological enzymes [12,13]. Compared with biological enzyme, nanozymes are less affected by the environment and can be stored stably, which have been widely used in medical and biological fields [12,14,15]. Chen's group proposed a sensitive colorimetric method for the detection of urine glucose based on the combination of the enzymatic reaction of GOD and etching of gold nanorods by H_2O_2 [16]. Xu *et al.* realized the detection of blood glucose based on enzyme-mediated etching of Au nanobipyramids [17]. Similar approaches have also been proposed using silver nanoparticles (NPs) [18], CeO_2 NPs [19], MoS_2 nanosheets [20] as nanozymes. These methods avoid the use of HRP, but GOD is still indispensable to initiate the enzymatic

* Corresponding author at: College of Science, China University of Petroleum (East China), Qingdao 266580, China.
E-mail address: zengjb@upc.edu.cn (J. Zeng).

https://doi.org/10.1016/j.cclet.2019.10.011
1001-8417/© 2019 Chinese Chemical Society and Institute of Materia Medica, Chinese Academy of Medical Sciences. Published by Elsevier B.V. All rights reserved.

reaction to produce H_2O_2. Therefore, the challenge of developing pure non-enzymatic glucose sensors has remained the driving force in many researches.

Noble metal nanomaterials that exhibit highly tunable localized surface plasmon resonance (LSPR) properties offer an excellent opportunity to construct sensitive colorimetric sensing applications [21]. Among various nanomaterials, Au NPs have been commonly reported to construct non-enzymatic glucose sensors [22]. Recent studies have shown that pony-size Au NPs have excellent GOD-like activity [23,24], which can be used as substitutes of GOD in glucose detection system. Meanwhile, silver nanomaterials have attracted great interest in recent years because of the properties of biocompatibility, strong shape-dependent optical properties and antibacterial properties [25]. Compared with Ag NPs, we noticed that Ag triangular nanoplates (Ag TNPs) exhibit better LSPR characteristics because of the high degree of anisotropy in their structures [26]. Moreover, Ag TNPs can be easily etched by hydrogen peroxide under enzymatic reaction [27]. However, Ag TNPs suffer from poor stability and easy oxidation, which to some extent decrease its attractiveness in practical application.

Based on these considerations, we deposit a thin layer of Au shells on the Ag TNPs by an epitaxial growth method to construct Ag@Au core/shell TNPs [28]. The introduction of Au shell not only enhances the stability of Ag TNPs, but also endows the material with GOD- and HRP-like dual nanozymes properties. In addition, the Ag TNPs can be used as signal transducers for visual readout. These two features make the Ag@Au core/shell TNPs viable candidates as nanoprobes for the colorimetric detection of glucose. Compared with the previous nanozymes-based glucose sensors, our method avoids the use of enzymes and organic chromogenic agent. The colorimetric assay developed was successfully applied to the determination of glucose in human urine, showing its great potential for on-site monitoring of glucose.

Fig. 1 schematically depicts the working principle of the assay based on the Ag@Au core/shell TNPs, which combines GOD- and HRP-like activities of Au shell and inherent shape- and morphology-dependent LSPR properties of Ag TNPs. It is hypothesized that, upon exposure of the nanoprobes to glucose, molecular oxygen is reduced to H_2O_2 by catalytic reaction of Au shell. Then, the generated H_2O_2 can be decomposed to $^{\cdot}OH$, which acts as an oxidant to etch the Ag TNPs into vacancies accompanied by a substantial decrease in absorbance.

Ag TNPs were firstly synthesized. As shown in Fig. 2a, the as-synthesized products are monodispersed with TNP-like structure. The spectra of these Ag TNPs were recorded using UV–vis. As shown in Fig. 2b, the products (blue curve) exhibit two main characteristic absorption peaks at around 330 nm and 750 nm

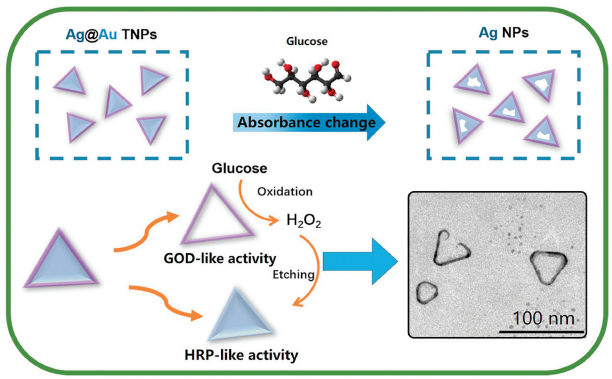

Fig. 1. Schematic illustration of the colorimetric detection of glucose based on Ag@Au core/shell TNPs.

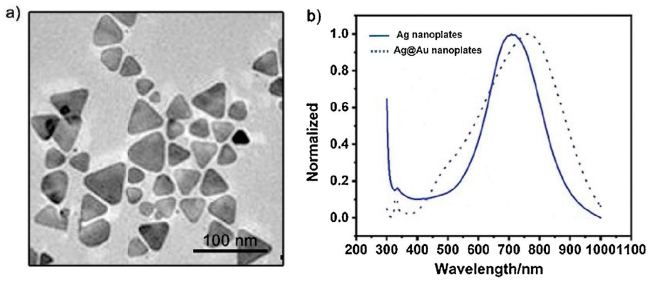

Fig. 2. Ag TNPs characterization: (a) TEM of the Ag TNPs; (b) UV–vis absorption spectra of Ag TNPs (blue curve) and Ag@Au TNPs (blue dotted curve).

arising from the in-plane dipole resonance and out-of-plane dipole resonance of TNPs, respectively, revealing the successful synthesis of Ag TNPs [26]. These Ag TNPs were used as seeds for the further deposition of Au shell by an epitaxial growth method. The synthetic Ag@Au TNPs were characterized using TEM, HRTEM, HAADF-STEM and EDX elemental mapping to get insights into their morphology, size and composition. Typical TEM images in Figs. 3a and b show that, a thin layer of shell with deeper contrast was deposited onto the Ag TNPs. HAADF-STEM characterization (Fig. 3 c) confirms again the formation of core/shell structure, in which a thin layer with a bright contrast is coated onto a TNP core with a darker contrast. Elemental mapping results (Figs. 3d–f) further evidence the shell and core belong to Au and Ag, respectively. Fig. 2 b shows that only a minor red shift was observed in the spectra for Ag@Au core/shell TNPs compared to that of Ag TNPs, indicating the layer of gold shell was not thick. As shown in Fig. S1 (Supporting information), the spectral absorption peak of pristine Ag TNPs decreased significantly after 5 days, while Ag@Au TNPs remain stable with only some minor changes observed after 15 days, revealing that Ag@Au core/shell structure offers better stability than the bare Ag TNPs

In order to explore the influence of gold shell thickness on the detection effect, gold shells of different thickness were deposited on the Ag TNPs by controlling the amount of $HAuCl_4$ (30, 50, 100, 200, 400 μL $HAuCl_4$) added. Three representative samples were characterized by TEM. As shown in Figs. 4a–c, by introducing incremental amounts of $HAuCl_4$, the thickness of Au shell continuously increases, which was 5.4 ± 0.6, 9.3 ± 0.9 and 13.2 ± 0.6 nm, respectively. Oxygen flow and incubation time were also optimized and set as 1 L/min and 25 min based on the results shown in Fig. S2 (Supporting information).

These Ag@Au core/shell TNPs with different shell thickness were added into the glucose solutions at the same concentration

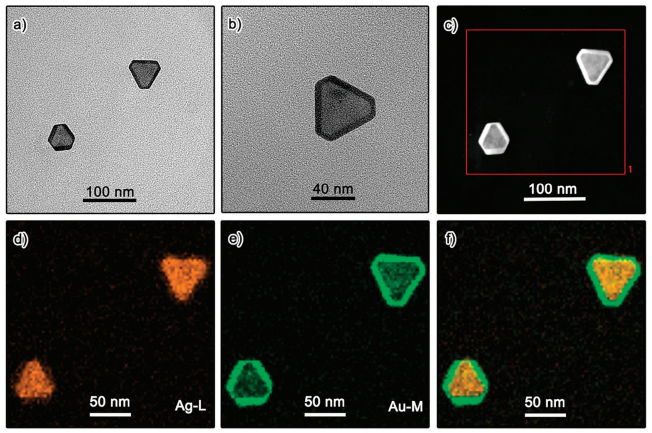

Fig. 3. (a, b) a HRTEM image, (c) corresponding HAADF-STEM image and (d, f) EDX elemental maps of synthetic Ag@Au triangle nanoplates.

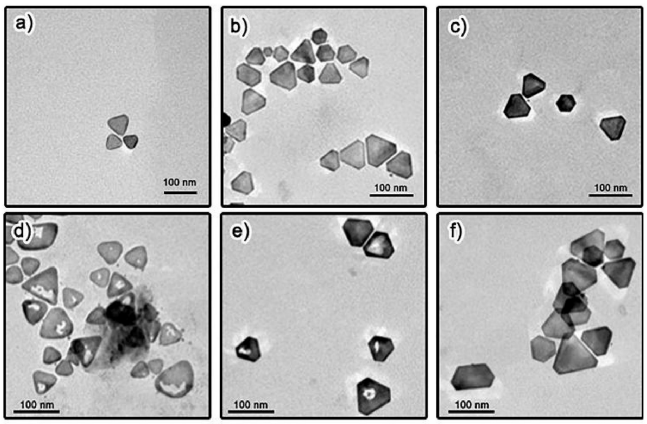

Fig. 4. TEM of the Ag TNPs upon reacting with different amount of $HAuCl_4$: (a) 50 μL, (b) 100 μL, and (c) 200 μL. Etched silver nanoplates formed by the reaction between silver nanoplates with different thickness of gold shells and glucose at the same concentrations: (d) 50 μL $HAuCl_4$; (e) 200 μL $HAuCl_4$; (f) 400 μL $HAuCl_4$.

and incubated with oxygen for 25 min. As shown in Fig. 4d, many vacancies were found in the core portion, indicating the silver cores were etched by the H_2O_2 generated by the catalytic oxidation of oxygen. With the increase of the thickness of Au shell, the vacancy in the Ag TNPs gradually decreases and the degree of etching gradually weakens, which indicates that the thickness of gold shell might affect the detection results (Figs. 4e and f). The inverse correlation between the thickness of gold shell and the degree of etching could be attributed to the thicker gold shell forms a dense protective layer on the surface of the silver TNPs, which is not conducive to the etching reaction. In addition, thicker gold shell probably leads to lower catalytic effect, which was also observed in the case of Au NPs with the relationship of particle size and GOD-like activity [29].

According to the mechanism of the reaction, gold shell thickness will affect the detection results. In order to better realize the accurate detection of glucose, the Ag@Au core/shell TNPs with different shell thickness were used to detect glucose. The results show that the Ag@Au TNPs with different thickness can be used to detect glucose, but with different response sensitivity and linear range. As shown in Figs. 5a and b, when higher concentration of $HAuCl_4$ was added in the nanoplates synthesis process, the Au shell was thicker, which produced color and spectral changes that were not conducive to observation. In contrast, as the amount of $HAuCl_4$ added decreased, the assay exhibited more obvious color and spectral changes, as shown in Figs. 5c–f. However, it should be noted that too little $HAuCl_4$ will lead to incomplete deposition of Au shell onto the Ag TNPs, which is also not beneficial for the detection of glucose. As shown in Figs. 5g and h, when 30 μL $HAuCl_4$ was added in the nanoplates synthesis process, inconspicuous color and spectral changes were observed. After considering the response sensitivity and linear range of the probe, the Ag@Au core/shell TNPs prepared by adding $HAuCl_4$ of 50 μL were used for the subsequent sensing experiments. The Ag@Au core/shell TNPs are with the core size and shell thickness of 51.2 and 5.4 nm, respectively, based on the TEM images shown in Fig. 4a.

As depicted in Figs. 5a and b, upon exposure to incremental concentration of glucose, the solution of the Ag@Au TNPs exhibited regular color changes from bright blue to colorless and the absorption peak decreased regularly at 800 nm. The lowest concentration of glucose that can be detected by naked eyes is 1 mmol/L. As illustrated in Fig. 6c, a good linear relationship was obtained between the ΔA value and glucose in the concentration range from 1 mmol/L to 30 mmol/L. The regression equation is

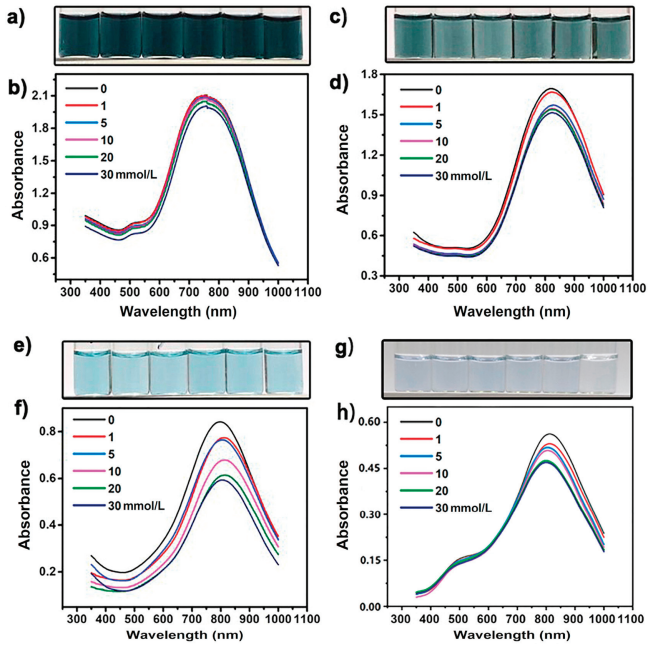

Fig. 5. UV–vis absorption images of Ag@Au TNPs with different gold-shell thicknesses to detect glucose: (b) 400 μL $HAuCl_4$; (d) 200 μL $HAuCl_4$; (f) 100 μL $HAuCl_4$; (h) 30 μL $HAuCl_4$; and (a, c, e, g) their corresponding digital photographs.

$\Delta A\ (nm) = 0.00325 \times [Glucose]\ (mmol/L) + 0.02469$ with a correlation coefficient of 0.988. The limit of detection (LOD) can reach 800 μmol/L, which was calculated by the equation of $LOD = 3\sigma/k$, where σ is the standard deviation of the control groups and k is the slope of the calibration graph. These results indicate that Ag@Au TNPs with thin gold shell has potential practicability for the analysis of glucose in real-life samples.

To evaluate its selectivity, the assay was used to analyze some typical chemical components possibly existing in the human urine. As indicated in Fig. 6d, 5 mmol/L of glucose can produce a visible decrease in absorbance at 800 nm. In contrast, no significant change in absorption peak was observed after the introduction of other components, all of which were with at least with 10-fold higher concentrations than that of glucose. Among these substances, $S_2O_3^{2-}$ has strong complexing ability and may etch Ag TNPs in the presence of oxygen [30]. Nevertheless, Ag@Au TNPs have little response toward $S_2O_3^{2-}$, proving that the proposed method has a high selectivity toward glucose.

To evaluate its viability for the analysis of glucose, the assay was applied to the determination of human urine collected from hospital of integrated Traditional and Western Medicine in Qingdao city. As shown in Table 1, the contents of glucose in these two samples are 4.1 and 5.2 mmol/L, which are similar to the reference value given by the hospital (2.6–5.5 mmol/L). Recovery tests were conducted to evaluate the reliability of the method. As summarized in Table 1, recoveries ranged from 90.2% to 103.0% and 96.5% to 102.3% in sample 1 and sample 2, respectively, indicating the proposed method is reliable and suitable for practical applications.

In summary, Ag@Au TNPs with thin gold shells were synthesized using an epitaxial growth method with the silver TNPs as the seed. The introduction of Au shell not only dramatically improves the stability of the Ag TNPs, but also provides excellent GOD-like activity for the subsequent glucose oxidation. The addition of glucose into the detection system initiated the glucose oxidation reaction to produce H_2O_2, which can etch the Ag TNPs and alter the LSPR characteristics of the Ag@Au TNPs structure. The change of LSPR characteristic leads to the significant change of its UV–vis

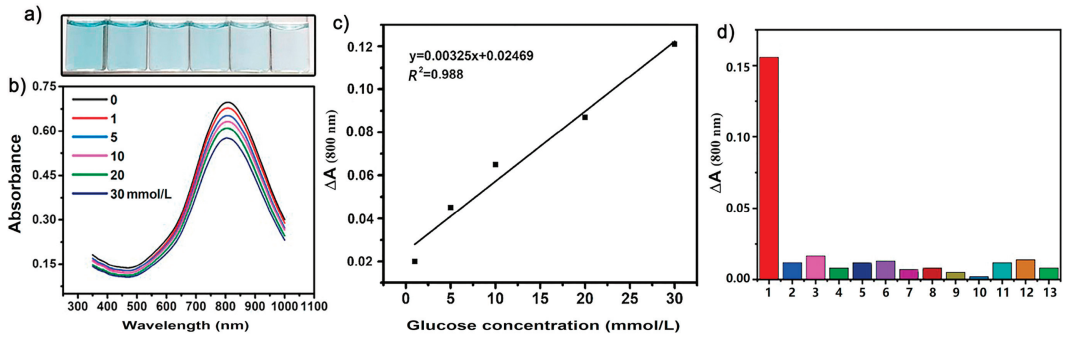

Fig. 6. (a) Photographs and (b) corresponding UV–vis absorption spectra of Ag@Au TNPs with different concentrations of glucose under optimized conditions. (c) Relationship between the absorption peak decline of test solution and glucose concentration. (d) The response of the colorimetric assay towards: 1. glucose (5 mmol/L); 2. carbamide (50 mmol/L); 3. NH_4^+ (50 mmol/L); 4. $S_2O_3^{2-}$ (50 mmol/L); 5. glycine (50 mmol/L); 6. histidine (50 mmol/L); 7. Ca^{2+} (70 mmol/L); 8. Mg^{2+} (70 mmol/L); 9. K^+ (70 mmol/L); 10. Na^+ (70 mmol/L); 11. S^{2-} (50 mmol/L); 12. SO_3^{2-} (50 mmol/L); 13. NO_3^- (50 mmol/L).

Table 1
Recoveries of the colorimetric assay for the detection of human urine added with different amounts of glucose.

Sample	Determined (mmol/L)	Added (mmol/L)	Detected (mmol/L)	Recovery (%)	Reference value (mmol/L)
1	4.1	5	8.6	90.2	+(2.6–5.5)
		10	14.4	103.0	
2	5.2	5	10.3	102.3	+(2.6–5.5)
		10	14.8	96.5	

absorption peak, thus realize the glucose colorimetric sensing without the presence of GOD. Therefore, this study provide an insight to the design of nanozyme-based colorimetric method, which holds great promise for the rapid detection of glucose with low cost, high stability and ease of operation.

Declaration of competing interest

The authors declare that they have no known competing financial interests or personal relationships that could have appeared to influence the work reported in this paper.

Acknowledgments

This work was supported by the National Natural Science Foundation of China (No. 21876206) and the Fundamental Research Funds for the Central Universities (No. 18CX02037A).

Appendix A. Supplementary data

Supplementary material related to this article can be found, in the online version, at doi:https://doi.org/10.1016/j.cclet.2019.10.011.

References

[1] A. Rawshani, A. Rawshani, S. Franzen, et al., N. Engl. J. Med. 376 (2017) 1407–1418.
[2] S. Beddhu, T. Greene, R. Boucher, et al., Lancet Diabetes Endocrinol. 6 (2018) 555–563.
[3] P.M. Seferovic, M.C. Petrie, G.S. Filippatos, et al., Eur. J. Heart Fail. 20 (2018) 853–872.
[4] C.P. Domingueti, L.M.S. Dusse, M.D. Carvalho, et al., J. Diabetes Complications 30 (2016) 738–745.
[5] D. Ziegler, N. Papanas, A. Zhivov, et al., Diabetes 63 (2014) 2454–2463.
[6] W.T. Cefalu, E.G. Berg, M. Saraco, et al., Diabetes care 42 (2019) S46-S60.
[7] M. Wooten, S. Karra, M.G. Zhang, W. Gorski, Anal. Chem. 86 (2014) 752–757.
[8] Z. Song, G.C. Fan, Z.M. Li, et al., Anal. Chem. 90 (2018) 10681–10687.
[9] J.Y. Sun, J.C. Ge, W.M. Liu, et al., Nanoscale 6 (2014) 255–262.
[10] X. Chen, J. Chen, F.B. Wang, et al., Biosens. Bioelectron. 35 (2012) 363–368.
[11] J.J.X. Wu, X.Y. Wang, Q. Wang, et al., Chem. Soc. Rev. 48 (2019) 1004–1076.
[12] Y.Y. Huang, J.S. Ren, X.G. Qu, Chem. Rev. 119 (2019) 4357–4412.
[13] X.Y. Lin, Y.F. Wang, M.M. Zou, T.X. Lan, Y.N. Ni, Chin. Chem. Lett. 30 (2019) 1157–1160.
[14] H.J. Cheng, L. Zhang, J. He, et al., Anal. Chem. 88 (2016) 5489–5497.
[15] L.Z. Feng, Z.L. Dong, C. Liang, et al., Biomaterials 181 (2018) 81–91.
[16] Z.Y. Zhang, Z.P. Chen, F.B. Cheng, Y.W. Zhang, L.X. Chen, Biosens. Bioelectron. 89 (2017) 932–936.
[17] S.H. Xu, L.P. Jiang, Y.Y. Liu, et al., Anal. Chim. Acta 1071 (2019) 53–58.
[18] H. Jiang, Z.H. Chen, H.Y. Cao, Y.M. Huang, Analyst 137 (2012) 5560–5564.
[19] M. Liu, Z.H. Li, Y.X. Li, J.J. Chen, Q. Yuan, Chin. Chem. Lett. 30 (2019) 1009–1012.
[20] T.R. Lin, L.S. Zhong, L.Q. Guo, F.F. Fu, G.N. Chen, Nanoscale 6 (2014) 11856–11862.
[21] O. Hess, J.B. Pendry, S.A. Maier, et al., Nat. Mater. 11 (2012) 573–584.
[22] J. Narang, N. Chauhan, C.S. Pundir, Analyst 136 (2011) 4460–4466.
[23] S. Choi, S.I. Han, D. Jung, et al., Nat. Nanotechnol. 13 (2018) 1048–1056.
[24] X.M. Shen, W.Q. Liu, X.J. Gao, et al., J. Am. Chem. Soc. 137 (2015) 15882–15891.
[25] X.J. Yue, T. Zhang, D.Y. Yang, et al., J. Colloid Interface Sci. 535 (2019) 363–370.
[26] Q. Zhang, N. Li, J. Goebl, Z.D. Lu, Y.D. Yin, J. Am. Chem. Soc. 133 (2011) 18931–18939.
[27] W.W. He, Y.T. Zhou, W.G. Wamer, M.D. Boudreau, J.J. Yin, Biomaterials 33 (2012) 7547–7555.
[28] H.P. Liu, T.Z. Liu, L. Zhang, et al., Adv. Funct. Mater. 25 (2015) 5435–5443.
[29] Y.H. Lin, J.S. Ren, X.G. Qu, Adv. Mater. 26 (2014) 4200–4217.
[30] J.J. Peng, G.K. Liu, D.X. Yuan, S.C. Feng, T.J. Zhou, Talanta 167 (2017) 310–316.